Novel Stemless Hip Prosthesis Design and Finite Element Analysis to validate stemless Prosthesis for Reduction of Aseptic Loosening in Total Hip Arthroplasty

Nishan Khadka[1*], Mukesh Yadav[2*], Adhish Ghimire[3]

[1]Department of Mechanical and Aerospace Engineering, Pulchowk Campus, Institute of Engineering, Tribhuvan University, Lalitpur, Nepal.
[2]Department of Mechanical Engineering, Delhi Technological University, New Delhi, India.
[3]Manipal Medical College, Kathmandu University, Pokhara, Nepal.
Corresponding: [1*]072bme626nishan@ioe.edu.np; [2*]mukesh7541@gmail.com

---

Abstract

Total Hip Arthroplasty/ Replacement is a major corrective procedure that involves replacing the head and neck of the femoral bone connected to the pelvis. Conventional methods involve long-stemmed Titanium Alloy (Ti_6Al_4V) implants with a Cobalt-Chrome (Co-Cr) spherical caps. The major problems that the current design presents are invasiveness, stress shielding due to the large distributions of interfacial stresses, and loosening and painful remission surgeries due to bone resorption, specifically in the younger and more active individuals. Thus, the need to improve upon the less invasive stemless models is warranted. This paper incorporates a comparative study between the natural femur, femur with the conventional implant, and a novel design using two prolongated probes fitted with a screw assembly. Finite element analysis of the design was performed on ANSYS software. The results concluded average induced stresses of 21.645 MPa, average strains of 0.002363 mm/mm, total deformation of 83.436 mm which were within close range compared to the conventional model and the natural femoral bone, for a point load of 2500N applied at an angle of 135° to the horizontal. Moreover, the results showed an improvement in fatigue life with more than 10^{10} cycles for the loading. The contact stresses also proved to be lesser and spread over a smaller area reducing the chances of aseptic loosening as compared to conventional models.

Keywords: Total Hip Arthroplasty, Hip prosthesis, Long-Stem implants, Stem-less implants, Finite Element Analysis, Aseptic Loosening, Stress Distribution

1.0 Introduction

The Hip joint is connected to one of the largest weight-bearing members of the human body. Naturally, the hip-joint forms a ball-socket joint, responsible for a wide range of motion and physical activities and weight-bearing functionality of the immediate area and parts of the neck, head, upper body, making it crucial in several static and athletic activities [1,2]. The Hip joint consists of a cup-shaped acetabulum supplied by a layer of lubricating synovial fluid. The acetabulum is connected to the pelvis which acts as the "socket" of the Hip joint. The femur's head is roughly spherical and fits comfortably in the Acetabulum, forming a Ball and Socket joint. The head of the femur is connected to the femoral neck, which is inclined (150° for children and <150° for adults) with respect to the femoral shaft (central lining of the femur bone) [1] connecting to the lower body. The assembly is supported by an assortment of ligaments [2].

The Hip joint is subjected to wear and tear, and even breakdown in the case of certain diseases like rheumatoid arthritis, osteoarthritis, fractures, and dislocations or fracture due to accidents [3]. The wear and tear of the Hip joint are however common with aging. Based on the severity of the bone's condition and the patient's biological information, Total Hip Replacement (THR) or Total Hip Arthroplasty (THA) could be recommended. THA or THR is the total replacement of the Ball and socket joint of the Hip with prosthetics materials like metal, ceramic, or plastic to rectify the problems associated with diseased or corrupted Hip joints [2]. THA is a prevalent procedure that aims to restore mobility with over 500,000 surgeries per annum projected in the US alone by 2030 [1] and more than a million procedures worldwide [4].

THA is a very intricate process as it involves the management of forces on the hip joint accounting for different motion ranges such as jogging, walking, running, jumping, etc [2]. In general, THA involves one of three methods based on the severity and patient's age. They are cemented methods (using cement of compounds like Methyl Methacrylate), Hybrid methods, and Non-cemented methods [23]. The most common method having an implant impinged into the femoral shaft or the femoral cavity [2]. Pioneered by Charnley in the 1960s, this method ubiquitous with THA's contemporary design and development. While the premise is entirely warranted for a successful THA, an invasive prosthesis elicits preventable problems in the future [24].

The major concerns regarding the invasive prosthesis or the conventional long-stemmed implants are that they lead to excessive stress shielding at the bone-implant contact region as well as thigh pains [6]. It has been observed that the prominent cause of the implant's failure is due to their aseptic loosening [9]. One of the reasons for aseptic loosening is "Osteolysis", which is the process of progressive destruction or disappearance of bone tissue [7], consequently leading towards the implant's failure. Microparticles are released from the femoral head when connected to the acetabular cup, leading to the progressive wear of the implant, causing osteolysis and resulting in aseptic loosening [6]. 10% of the patients with THR are needed revision surgery within 10 years, with an average life-span of is 15 years. Revision surgery may lead to inoperable fractures [10]. It has been observed that the revision surgery is substantially more complicated than the initial surgery as the previous implant needs to be removed, making it a very complicated process [7]. Moreover, the patients are more susceptible to complications with longer recovery time, making it a riskier process, costly and inconvenient. [8,9]. Thus, efforts are made to make prosthetics life longer. Although, long-stemmed prosthesis doesn't have many issues for the elderly; however, problems such as aseptic loosening and fracture make it highly inconvenient for the youth (<60) [29].

The typical design of THA prosthesis in contemporary medicine consists of " a femoral stem, a femoral head (ball) (that attaches to the stem), an acetabular cup, and a fixation agent to secure the implant's stem into the femur and the femoral head into the acetabular cup of the pelvis" [5]. For the qualification of the implant's invasiveness and reduced remission surgeries, different stemless and short-stemmed designs have emerged [23]. The short-stemmed design has been excellent in improving the load transfer and circumventing some of the major problems incurred by invasive long-stemmed implants, making it a suitable design for youth [11,4,12]. Munting and

Verphelen [13] introduced a short rod implant with several bolts for fixation. This step towards mitigating the problem of invasiveness was positive but was curtailed by the use of metal bolts on brittle bones. The stemless design addressed the biocompatibility question by Suresh G. Advani et al [11], where belts were used for fixation. This paper intends to improve upon the previous designs of the stemless hip prosthesis while being objective about the reduction of stress shielding and aseptic loosening. Therefore, a comparative study has been conducted by using Finite Element Methods

2.0 Methodology

2.1 Design

The proposed hip prosthesis was based on previous stemless designs by Advani S, [14] and Munting and Verphelen [13]. The CAD models were created on SolidWorks 2018. The femur's CAD file was imported from GrabCAD [18], which incorporated a CAM based on CT scan imaging of an actual femur [15]. The models used in this study included: - (a) the CAD model of the femur as a control group, (b) the conventional stemmed (Ti6AI4V) prosthesis [19], and (c) the proposed novel stemless model.

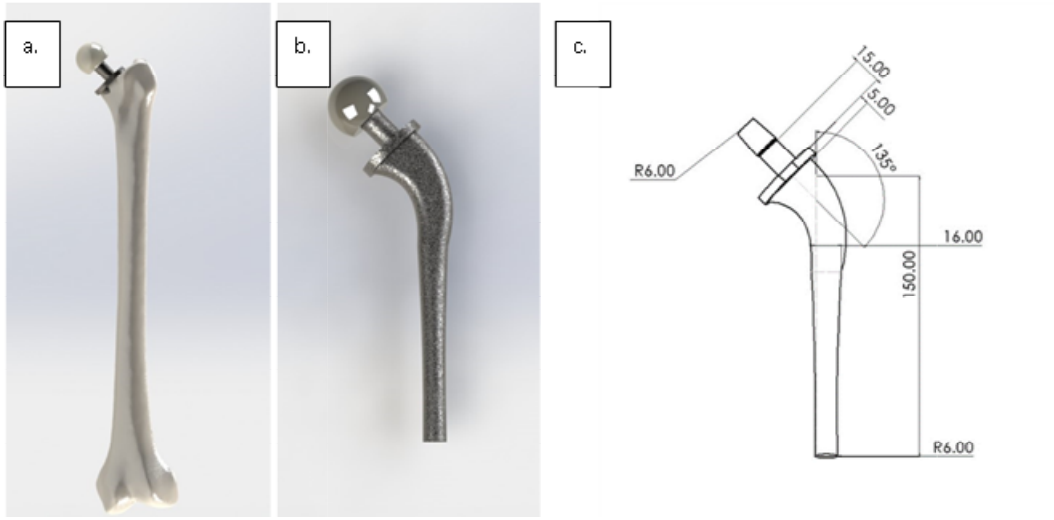

Figure 1 **a)** 3D model of the conventional prosthesis implanted into the femoral cavity **b)** 3D model rendering of the conventional prosthesis [15,20] consisting of the acetabular head **c)** 2D drawing of the CAD model of the prosthesis highlighting salient dimensions in mm.

SolidWorks 2018 was used as the primary CAD software to model the prosthesis. The contemporary design of the prosthesis consisted of an acetabular cup made from Cobalt-Chrome (Co-Cr), which fitted into the acetabular cavity (acetabulum) of the pelvic bone. [1]. The rest of the prosthesis consisted of a Titanium Alloy (Ti6Al4V) stemmed implant, which was the modification of Charnely's original prosthesis [15]. The acetabular cup was a sphere of 16mm radius, which lead to a femoral neck (implant neck) of 12 mm diameter, 15mm at thickest, 15mm

in length, and was connected to the implant's stem banked at 135° [1]. The stem was 16mm at its thickest (proximal end) and 12mm at the distal end [15,20]. The 3D model is represented in fig 1.

The proposed novel design comprised changes made to the original Munting and Verphelen [13] and the Advani S, [14], except the short-stem was replaced by two small diameters (~4mm probes). The implant consisted of an acetabular cup (16mm spheroid), which is to be placed in the pelvis's acetabulum, similar to the conventional stemmed design. It leads to a short neck of 15mm in length and 10mm in diameter. The neck connected to the flat plate similar to the stemmed prosthesis but was broader. The plate's distal part consisted of two 4mm diameter probes separated by 12mm, which was internally threaded (2mm internal diameter) along its length of 40mm, as seen in fig. 2d. and 2e. An 18×5×2mm plate with 2×2mm diameter holes at the extremes was provided to secure the implant with the help of M2 Polyurethane ANSI metric 18.36 countersunk screws. The plate was placed on the small space between the Quadratus femoris and the iliopsoas muscle; a small 15mm cavity was made on the femur. The design was made to allow the screws to fit inside the internally threaded probes. The use of screws along with the minimal invasion of the femur helped the implant to secure onto the femur.

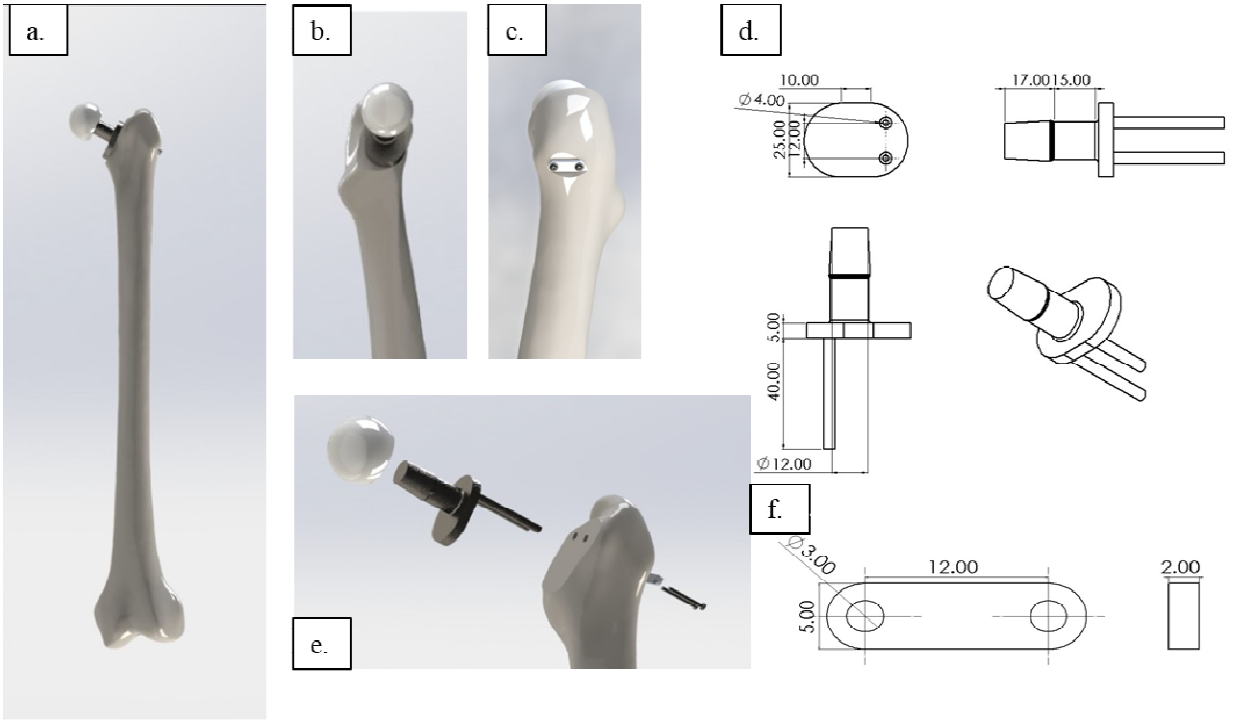

Figure 2 **a)** 3D model rendering of the proposed no-stem prosthesis design affixed onto the femur **b)** Back View of the proposed no-stem prosthesis design with the femur **c)** Front View of the proposed no-stem prosthesis design with the femur **d)** 2D drawing of the implant model with dimensions in mm. **e)** 3D model rendering of the proposed no-stem implant with acetabular head.

The implant body in both cases was made up of the conventional Ti6Al4V alloy. The acetabulum was made up of ceramic, which fitted over the implant's neck. The use of lateral screws was intended to remove the invasiveness associated with Muting's designs [13], and the small probes

were intended to reduce loosening prevalent in Advani S's design [14]. Further, the use of polyurethane sockets and screws were assumed to eliminate bio-compatibility issues with affixation [30]. The illustrations are represented in fig 2.

2.2 Numerical methods

The finite element analysis of the three groups was carried out using ANSYS 2019. The control group was taken as a standard femoral bone [4], while study group 1 included a conventional prosthesis model based on modified Charnely's [13] stemmed prosthesis, as shown in fig 1. The proposed model or study group 2 comprised of the stemless model fixed onto the femur as shown in fig 2. The primary study area included static analysis viz. deformation under the loading conditions, Von-Mises Stresses, Total Elastic Strain, and fatigue under cycling loading conditions. The study aimed to determine the proposed model's integrity for its qualification as the suitable hip prosthesis with a conventional counterpart within the extreme limits of loading conditions.

2.2.1 Materials and Method

Isotropic properties were considered in the FEA of all the study groups. To perform the FEA, properties such as density, Young's Modulus of Elasticity (GPa), and Poisson's ratio needed to be addressed. Further, for the analysis of fatigue life, properties such as Yield Strength and the tentative Stress-Total Life to failure (S-N) curve data were required. The relevant data has been tabulated in Table 1.

The human bone comprises a mineral composition of organic and inorganic materials like hydroxyapatite and water. They can be broadly classified into cortical bones, ligaments, cancellous bone, and cartilage. Median values of the isotropic properties of materials were considered [21].

Table 1 Materials used in the 3D model's FEA along with its isotropic properties of Young's modulus of elasticity Poisson's Ratio, and Compressive Yield Strength

Components	Materials	Elastic Modulus (GPa)	Yield Strength (GPa)	Poisson's Ratio
Femoral Stem and Metal Shell	Titanium Alloy Ti_6Al_4V	110	0.88	0.32
Femoral head Inner liner (acetabular cap)	Cobalt-Chrome (Co-Cr)	220	0.76	0.31
Bone	Collagen+ calcium phosphate	10	0.15	0.15
Screws	Glass-fiber reinforced Polyurethane	72.3	1.95	0.2

In the implant, Cobalt-Chrome was used as the acetabular head's material, while the body of both the stemmed implant and stemless implant was made up of Titanium alloy (Ti6Al4V). For the stemless implant, the fixation method involved the use of glass-reinforced polyurethane screws [31,32]. The properties of the materials have been shown in table 1

2.2.2 Loading Conditions

The femur head and the neck were assumed to be rigid bodies to improve computational efficiency. The average human of 1.7m in height weighs about 75 kg or 735N. In a one-legged stance, the human hip naturally can support three times its weight without any aggressive damage to the hip joint [16]. Therefore, a load equivalent to ~(735×3N) or assume, for redundancy, 2500N was applied to the acetabular cup in either case in the X- horizontal and Y-vertical axis direction. A net equivalent force acted along the femoral neck axis in either the natural bone, stemmed, or stemless implant, i.e., 135° with the horizontal. Loads in the z-axis were avoided deliberately to simplify the calculation as they are minimal as compared to x and y axes, also it helps to maintain the implant and bone deformation in the 2D plane.

For supports, musculature was not considered to evade complications. Rigid support was applied at the distal end of the long bone, which signifies the beginning of the human anatomy's knee joint [1].

2.2.3 Setting up for FEM

The control group was affixed onto the XY plane with its central axis parallel to SpaceClaim's y-axis. For study group 1, the contact zones were defined; the acetabular cup bonded with the implant's femoral neck, and the contact region of the stem of the implant and the femoral cavity were considered rough surfaces in the Mechanical Modeler. The proposed stemless design was similarly modeled in ANSYS. Contact between the implant's inner parts with the femur was considered rough surfaces.

Each study group was meshed with default triangular elements of the mechanical modeler with increased mesh density at the plane of contact to avoid convergence errors in the ANSYS solver and obtain a degree of accuracy in the salient regions. The mesh quality details have been tabulated in table 2, and the Meshed images have been shown in Fig 3.

Table 2 Statistics of Mesh in terms of the number of nodes and elements in the respective study group.

Model	Number of Nodes	Number of Elements
Conventional model in the femur	61357	34834
Femur without an implant (control)	31056	17630
Proposed stemless design	40442	21233

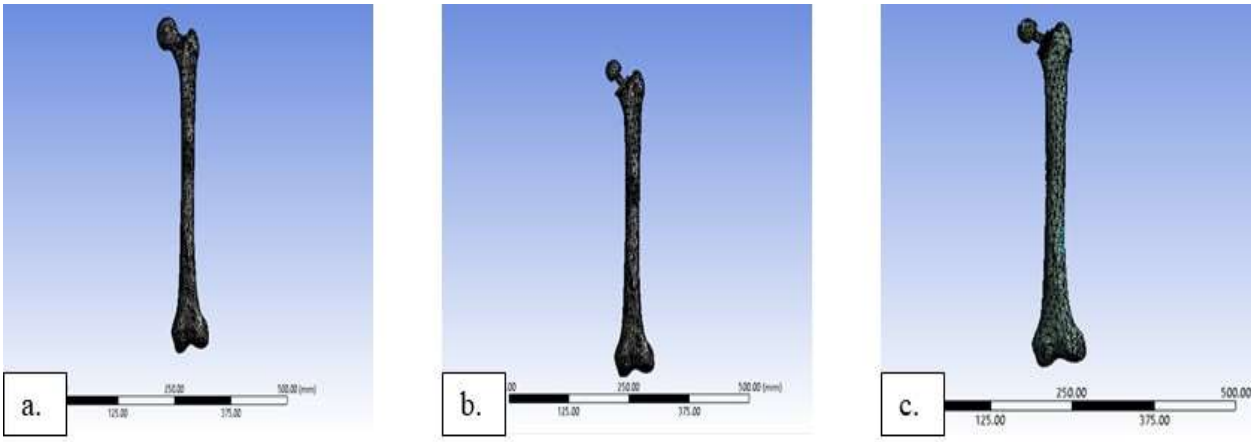

Figure 3 **a)** 3D model of the meshed femur (control) **b)** 3D model of the meshed conventional stem hip prosthesis **c)** 3D model of the meshed proposed stemless hip prosthesis

3.0 Results & Discussion

The static structural analysis of the hip joint was carried out for the three different study groups a) femur bone (control group), b) conventional stemmed hip prosthesis implanted on the femur c) Proposed stemless hip prosthesis affixed on the femur. The FEA of each model is represented from fig 4 to 9.

3.1 Total Deformation

The prosthesis and the control group subjected to the boundary conditions as stated in 2.2.2 showed some amount of deformation, which has been tabulated in Table 3, and the deformation plots have been represented in fig 4.

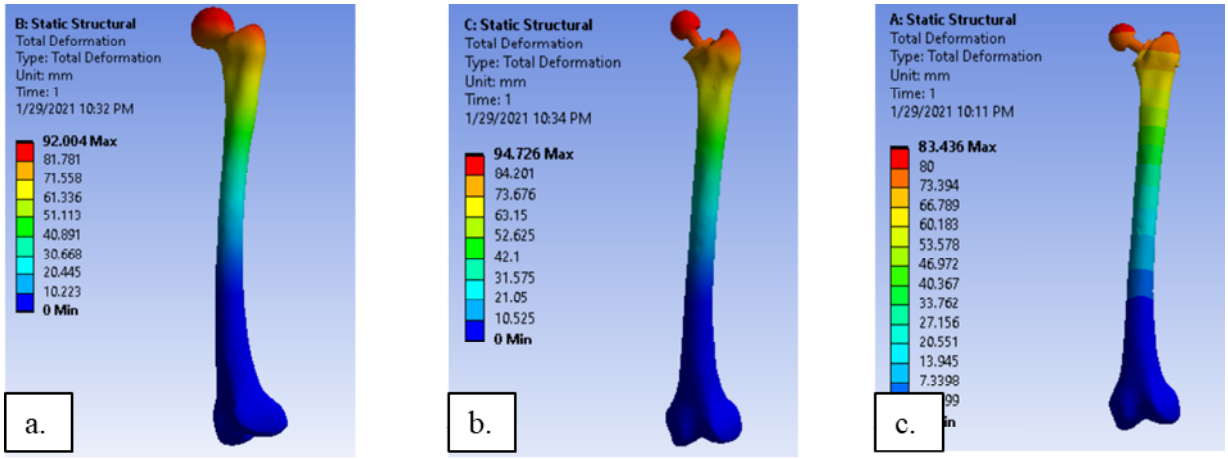

Figure 4 Total deformation plot of **a)** Natural Femur(control) **b)** Conventional stemmed hip prosthesis implanted onto the femur **c)** proposed stemless hip prosthesis affixed onto the femur.

It can be seen that the maximum deformation occurs at the femoral head of the bone, represented by the red region, which gradually decreases towards the bottom. The magnitude of the range of deflection is represented in table 3. The proposed stemless implant has a maximum deflection of 83.436 mm, which is less compared to the conventional stemmed implant (94.736 mm) and the control group i.e. the natural femoral bone (92.078 mm). Incidentally, deformation is also mainly nearing the top of the proximal part of the femur. This is also common to the uppermost part of the implant in the stemless model. From the results of static analysis of the conventional stemmed implant, it can be seen that the maximum deformation is observed in the head region of the implant, similar to the results seen in the analysis of the natural femur. This could be because of the concentrated load being applied at that point in the implant, which is not common in practical application [25]. However, extreme data is warranted for the study.

Table 3 Range of displacement from Total Deformation plot in the respective study group

Model	Maximum displacement(mm)	Minimum displacement(mm)
Femur without implant (control)	92.078	0
Conventional model in the femur	94.726	0
Proposed stemless design	83.436	0

Total or Equivalent Stresses

The maximum von-mises stress can be seen in the bone's shaft in all three study groups. The stress-induced in the plane plate of the proposed design is also well within limits. It was seen that stress concentrations existed in the stemless implant's fixation area, with a maximum magnitude of 363.58 MPa but is lower than the maximum stress observed in the conventional model for the same boundary conditions. The stress distribution is represented in Figure 4 where a range of stress is represented by the color contour in the figure.

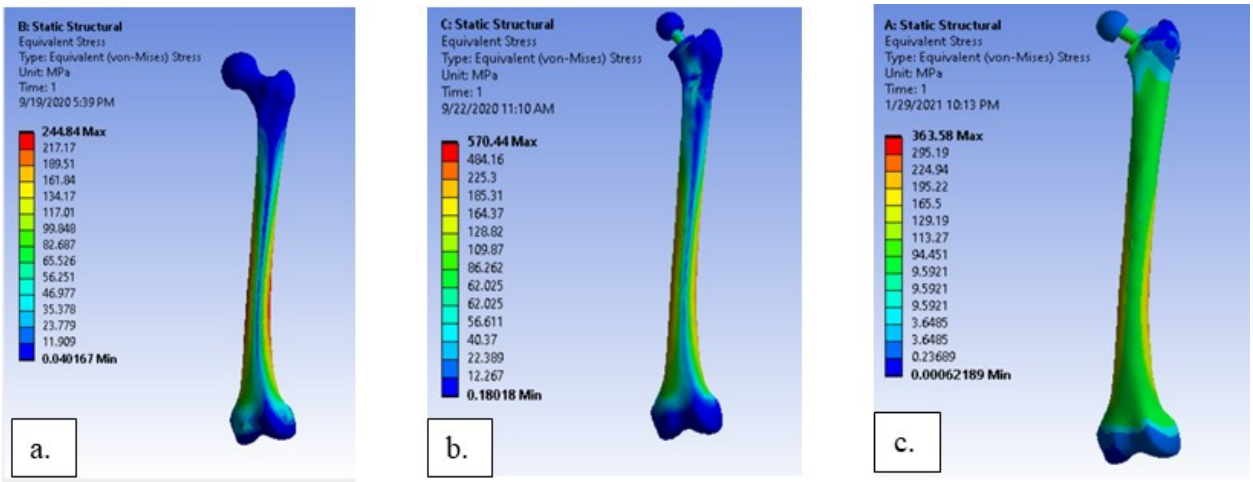

Figure 5 Total or Equivalent (von-Misses) Stress plot of **a)** Natural Femur(control) **b)** Conventional stemmed hip prosthesis implanted onto the femur **c)** proposed stemless hip prosthesis affixed onto the femur.

The static analysis of the proposed stemless implant showed similar results for the deformation as in the previous designs. The stress distribution, however, with the use of probes can be seen greater in the areas of fixation i.e. the polyurethane screws. This could be due to the presence of localized stresses in a relatively small area of fixation [26].

Table 4 Range of displacement from Total Deformation plot in the respective study group

Model	Maximum stress (MPa)	Average Stress (MPa)	Minimum stress (MPa)
Femur without implant (control)	244.84	38.672	0.007292
Conventional model in the femur	570.44	25.628	0.18018
Proposed stemless design	363.58	21.645	0.00062

From table 4, it was seen that the average stress was the lowest in the proposed stemless model as compared to the conventional model and the femur bone (control group). This implies that the stress-induced in the proposed design is not large enough to cause any appreciable damage compared to the conventional model.

Equivalent Strain

The plot of the equivalent strain in each of the study group is represented in fig 6. The values of strain are tabulated in table 5.

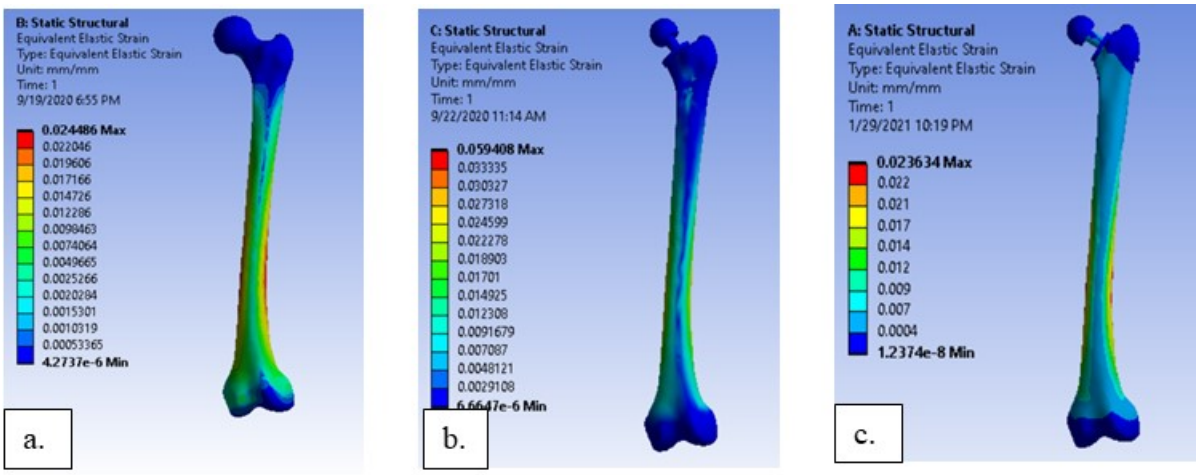

Figure 6 Total or Equivalent Elastic Strain plot of **a)** Natural Femur(control) **b)** Conventional stemmed hip prosthesis implanted onto the femur **c)** proposed stemless hip prosthesis affixed onto the femur.

The values of maximum strain in femur bone (control group) and the proposed design are comparable. However, maximum strain in the conventional design had an expected high value because of the induced localized stresses as discussed above [26]. Moreover, the maximum strain was observed at the femoral shaft in each design.

Table 5 Range of displacement from Total Deformation plot in the respective study group

Model	Maximum strain (mm/mm)	Average Strain(mm/mm)	Minimum strain (mm/mm)
Femur without implant (control)	0.0244	0.0038	4.2736×10^{-6}
Conventional model in the femur	0.0594	0.00259	6.6647×10^{-6}
Proposed stemless design	0.023634	0.002363	1.27×10^{-8}

The average strain for the proposed stemless design is more significant than the least valued standalone femur and the comparable conventional model. The biggest drawback is the localized strain in the new model; however, the average values are within the limit [16].

Fatigue Life Analysis

Fatigue life analysis of the analysis was also conducted for the conventional stemmed implant, and the proposed stemless implant with load considered a reversed cyclic load. The Total life plot of each implant is presented in fig 7.

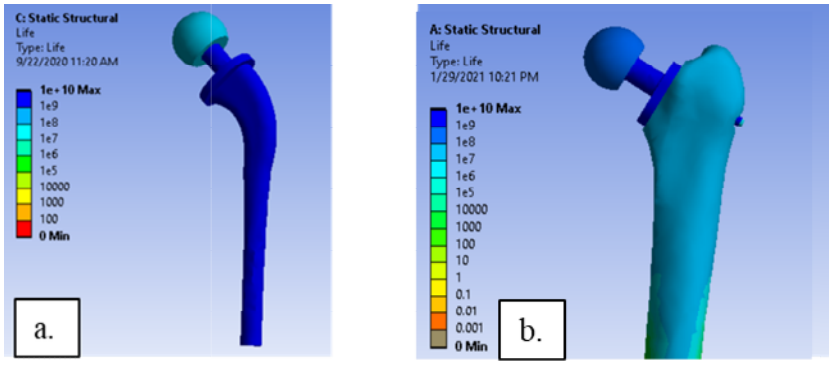

Figure 7 Fatigue life distribution plot of **a)** Conventional stemmed hip prosthesis **c)** proposed stemless hip prosthesis affixed onto the femur.

From the result, it was observed that the life of the stemless implant was very comparable to the conventional model in terms of fatigue failure. The issue with the conventional model was with a lower life for the Co-Cr head while the polyurethane screws have a slightly lower life in the proposed design.

Contact stresses

The contact stress distribution is an important factor in the analysis of aseptic loosening [31]. The contact frictional stress distribution has been shown for both the conventional hip prosthesis model and the proposed stemless hip prosthesis.

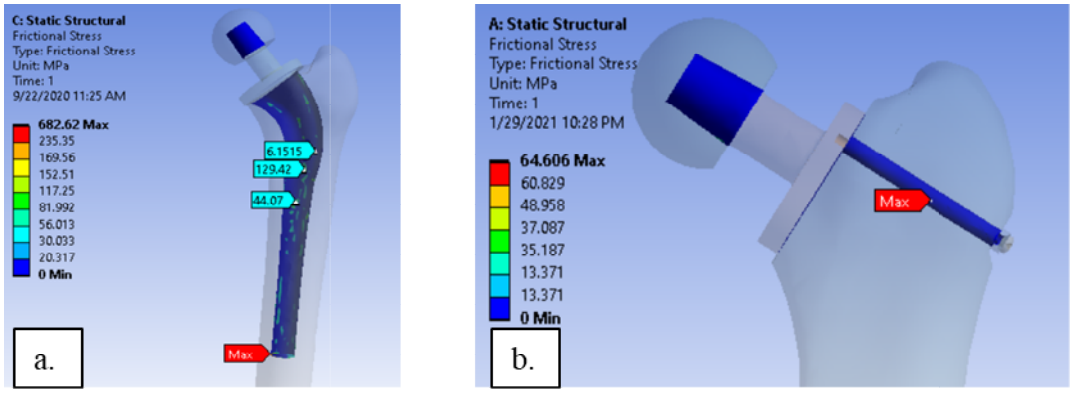

Figure 8 Contact stress distribution plot of **a)** Conventional stemmed hip prosthesis **c)** proposed stemless hip prosthesis affixed onto the femur.

The conventional model relied on a significant contact area while the proposed model had lesser contact. The proposed design was secured using the screws while the conventional implant relied on cemented or uncemented contact between the cancellous and cortical Femoral cavity of the long bone [25].

As the result suggested, the conventional model had an unusual stress range for the same boundary conditions. The maximum contact stress is roughly 700MPa for the conventional model and is distributed with localized stress. However, the distribution of the stemless implant had a lower magnitude of maximum contact stress and fewer spots of localized stresses [26]. The effect of stress shielding is common with higher interfacial stresses and with a larger contact area, conventional models are prone to bone resorption and consequently aseptic loosening [32].

Conclusions

The new stemless model for hip prosthesis was successfully created based on the older stemless designs' efficacy and shortcomings. The novel prosthesis was analyzed for stress distributions, deformation, strain, fatigue life, and interfacial stresses using FEA, and the results were compared with the FEA of standalone Femur as a control group and the conventional design of the long-stemmed hip prosthesis.

The FEA yielded reduced deformation compared to that of the other study group at around 7.27 mm for an excessive force of thrice the bodyweight of a human being (87kg). The results were followed by average stress distributions of approximately 21.645 MPa in an appropriate range (~minimal- 363.58MPa), which was a good value compared to the other study groups. This was also the case for strain distribution as both range, and average values were lower than the conventional and comparable to the natural bone. The fatigue life was much better with the new prosthesis as compared to the conventional model and the contact stresses induced minimal contact with proper stress distribution, which compared to the high valued, broad surface stress distribution of the conventional model was better at reducing stress shielding and subsequently bone resorption and aseptic loosening [28]. Further, the minimally invasiveness and ease of access during remission surgeries favor the proposed design.

The design would stand as a better, less invasive, more durable alternative. However, further studies are warranted to validate its feasibility. The use of biocompatible material with a compact design will reduce localized stresses and prevent failures and preclude blood toxicity. Also, better fixation methods will be conducive to perpetuating the stemless implant ideology as a staple form of prosthesis, especially for the active individual.

References

1. Byrne, Damien P, Kevin J Mulhall, and Joseph F Baker. 2010. "Anatomy & Biomechanics of the Hip." *The Open Sports Medicine Journal*. Vol. 4. DOI: 10.2174/1874387001004010051
2. Sathishkumar, S, M Sivasankar, S Arunkumar, V Bakkiyaraj, and A Muruganandam. 2016. "A Review on Total Hip Replacement." DOI: 10.13140/RG.2.2.13686.80969.
3. Kurtz, Steven, Kevin Ong, Edmund Lau, Fionna Mowat, and Michael Halpern. 2007. "Projections of Primary and Revision Hip and Knee Arthroplasty in the United States from 2005 to 2030." *Journal of Bone and Joint Surgery - Series A* 89 (4): 780–85. DOI: 10.2106/JBJS.F.00222.
4. Derar, H, and M Shahinpoor. 2015. "Recent Patents and Designs on Hip Replacement Prostheses." *The Open Biomedical Engineering Journal* 9 (1): 92–102. DOI: 10.2174/1874120701509010092.
5. Clarke A, Pulikottil-Jacob R, Grove A, et al. Total hip replacement and surface replacement for the treatment of pain and disability resulting from end-stage arthritis of the hip (review of technology appraisal guidance 2 and 44): systematic review and economic evaluation. Southampton (UK): NIHR Journals Library; 2015 Jan. (Health Technology Assessment, No. 19.10.) Chapter 1, Background. Available from: https://www.ncbi.nlm.nih.gov/books/NBK273961/
6. Zebolds, S. and Jumtins, A., 2010. The Evaluation of Early Results after Total Hip Replacement in Dysplastic Hip Patients. *Acta Chirurgica Latviensis*, 10(2).
7. Saleh, K. and Schwarz, E., 2004. Osteolysis. *Clinical Orthopaedics and Related Research*, 427, pp.138-147.
8. Trivedi,, V., Goel, Y., Singh, R., Khan, Y., Mishra, A. and Qidwai, S., 2018. Single Stage Cementless Bilateral Total Hip Replacement Surgery: Case Report and Review of Literature. *Era's Journal of Medical Research*, 5(2), pp.204-207.
9. Sherry, E., Egan, M., Warnke, P., Henderson, A. and Eslick, G., 2003. Minimal invasive surgery for hip replacement: a new technique using the NILNAV hip system. *ANZ Journal of Surgery*, 73(3), pp.157-161.
10. Sargeant, A., and T. Goswami. 2006. "Hip Implants: Paper V. Physiological Effects." *Materials and Design* 27 (4): 287–307. DOI: 10.1016/j.matdes.2004.10.028.
11. Bergmann, G., F. Graichen, and A. Rohlmann. 1993. "Hip Joint Loading during Walking and Running, Measured in Two Patients." *Journal of Biomechanics* 26 (8): 969–90. DOI: 10.1016/0021-9290(93)90058-M.
12. Logroscino, Giandomenico, Fabrizio Donati, Vincenzo Campana, and Michela Saracco. 2018. "Stemless Hip Arthroplasty versus Traditional Implants: A Comparative Observational Study at 30 Months Follow-Up." *HIP International* 28 (2_suppl): 21–27. DOI: 10.1177/1120700018813209.
13. Munting, E., and M. Verhelpen. 1995. "Fixation and Effect on Bone Strain Pattern of a Stemless Hip Prosthesis." *Journal of Biomechanics* 28 (8). DOI: 10.1016/0021-

9290(94)00146-U.
14. S.G. Advani, M.H. Santare, F. Miller, and M. Joshi. 2002, “Stemless hip prosthesis”, U.S. Patent 6,379,390 B1.
15. Rawal, B R & Ribeiro, Rahul & Malhotra, Rajesh & Bhatnagar, N. 2011. Design and Manufacture of Short stemless Femoral Hip Implant based on CT Images. Journal of Medical Sciences (Faisalabad). 11. 296-301. DOI: 10.3923/jms.2011.296.301.
16. Asgari, S. & Hamouda, A.M.S & Mansor, Shattri & Singh, Harwant & Mahdi, Elsadig & Wirza, Rahmita & Prakash, B. 2004. Finite element modeling of a generic stemless hip implant design in comparison with conventional hip implants. *Finite Elements in Analysis and Design - Finite Elemental Design*. 40. 2027-2047. DOI: 10.1016/j.finel.2004.02.003.
17. Yan, Shuang G., Yan Chevalier, Fanxiao Liu, Xingyi Hua, Anna Schreiner, Volkmar Jansson, and Florian Schmidutz. 2020. “Metaphyseal Anchoring Short Stem Hip Arthroplasty Provides a More Physiological Load Transfer: A Comparative Finite Element Analysis Study.” *Journal of Orthopaedic Surgery and Research* 15 (1). DOI: 10.1186/s13018-020-02027-4.
18. Isaza, E. García, L. and Salazar, E. 2015. “Determination of Mechanic Resistance of Osseous Element through Finite Element Modeling”.
19. Chao, Jesús, and Víctor López. 2007. “Failure Analysis of a Ti6Al4V Cementless HIP Prosthesis.” *Engineering Failure Analysis* 14 (5): 822–30. DOI: 10.1016/j.engfailanal.2006.11.003.
20. Mughal, Uzair N., Hassan A. Khawaja, and M. Moatamedi. 2015. “Finite Element Analysis of Human Femur Bone.” *International Journal of Multiphysics* 9 (2): 101–8. DOI: 10.1260/1750-9548.9.2.101.
21. Filipovic, N. (2020). The biomechanics of lower human extremities. *Computational Modeling in Bioengineering and Bioinformatics, 179–210.* DOI:10.1016/b978-0-12-819583-3.00006-0.
22. Jung, Jin Mu, and Cheol Sang Kim. 2014. “Analysis of Stress Distribution around Total Hip Stems Custom-Designed for the Standardized Asian Femur Configuration.” *Biotechnology and Biotechnological Equipment* 28 (3): 525–32. DOI: 10.1080/13102818.2014.928450.
23. Ghanem, M., Farag, M., Schneider, P. 2013. The short stem GHEs in total hip replacement – experience after 380 implantations. *Gms Interdiscip Plast Reconstr Surg Dgpw*.
24. Hwang, Sung Kwan. 2014. “Experience of Complications of Hip Arthroplasty.” *Hip & Pelvis* 26 (4): 207. DOI: 10.5371/hp.2014.26.4.207.
25. Bergmann, Georg, Alwina Bender, Jörn Dymke, Georg Duda, and Philipp Damm. 2016. “Standardized Loads Acting in Hip Implants.” *PLoS ONE* 11 (5): 1–23. DOI: 10.1371/journal.pone.0155612.
26. Fakhouri, Sarah Fakher, Marcos Massao Shimano, Cleudmar Amaral de Araújo, Helton Luiz Aparecido Defino, and Antônio Carlos Shimano. 2014. “Analysis of Stress Induced by Screws in the Vertebral Fixation System.” *Acta Ortopedica Brasileira* 22 (1): 17–20. DOI: 10.1590/S1413-78522014000100002.
27. Kutzner, Ines, Geir Hallan, Paul Johan Høl, Ove Furnes, Øystein Gøthesen, Wender Figved, and Peter Ellison. 2018. “Early Aseptic Loosening of a Mobile-Bearing Total Knee

Replacement: A Case-Control Study with Retrieval Analyses." *Acta Orthopaedica* 89 (1): 77–83. DOI: 10.1080/17453674.2017.1398012.

28. Ridzwan, M. I.Z., Solehuddin Shuib, A. Y. Hassan, A. A. Shokri, and M. N. Mohammad Ibrahim. 2007. "Problem of Stress Shielding and Improvement to the Hip Implant Designs: A Review." *Journal of Medical Sciences* 7 (3): 460–67. DOI: 10.3923/jms.2007.460.467.
29. Wangen, H., P. Lereim, I. Holm, R. Gunderson, and O. Reikerås. 2008. "Hip Arthroplasty in Patients Younger than 30 Years: Excellent Ten to 16-Year Follow-up Results with a HA-Coated Stem." *International Orthopaedics* 32 (2): 203–8. DOI: 10.1007/s00264-006-0309-2.
30. Joshi, Makarand G., Suresh G. Advani, Freeman Miller, and Michael H. Santare. 2000. "Analysis of a Femoral Hip Prosthesis Designed to Reduce Stress Shielding." *Journal of Biomechanics* 33 (12): 1655–62. DOI: 10.1016/S0021-9290(00)00110-X.
31. Properties: E-Glass Fibre. (2020). Retrieved 22 September 2020, from https://www.azom.com/properties.aspx?ArticleID=764.
32. Elsner, Jonathan & Eliaz, Noam & Linder-Ganz, Eran. 2015. The Use of Polyurethanes in Joint Replacement. DOI: 10.1142/9781783267170_0009.